CODEN IEJMAT *Internet Electronic Journal of Molecular Design* **2009**, *8*, 14–28 ISSN 1538–6414
BioChem Press http://www.biochempress.com

Inter*net* Electronic Journal of Molecular Design

January 2009, Volume 8, Number 2, Pages 14–28

Editor: Ovidiu Ivanciuc

Design of New Chemicals Entities as Selective COX–2 Inhibitors using Structure Optimization by Molecular Modeling Studies

Shashikant Bhandari,[1] Kailash Bothara,[1] Vidya Pawar,[1] Deepak Lokwani,[1] and Titiksh Devale [1]

[1] A.I.S.S.M.S. College of Pharmacy, Kennedy Road, Pune–411001, Maharashtra, India

Received: May 9, 2009; Revised: September 27, 2009; Accepted: November 9, 2009; Published: November 26, 2009

Citation of the article:
S. Bhandari, K. Bothara, V. Pawar, D. Lokwani, and T. Devale, Design of New Chemicals Entities as Selective COX–2 Inhibitors using Structure Optimization by Molecular Modeling Studies, *Internet Electron. J. Mol. Des.* **2009**, *8*, 14–28, http://www.biochempress.com.

Inter*net* **Electronic** Journal of Molecular Design

BioChem Press
http://www.biochempress.com

Design of New Chemicals Entities as Selective COX–2 Inhibitors using Structure Optimization by Molecular Modeling Studies

Shashikant Bhandari,[1,*] Kailash Bothara,[1] Vidya Pawar,[1] Deepak Lokwani,[1] and Titiksh Devale [1]

[1] A.I.S.S.M.S. College of Pharmacy, Kennedy Road, Pune–411001, Maharashtra, India

Received: May 9, 2009; Revised: September 27, 2009; Accepted: November 9, 2009; Published: November 26, 2009

Internet Electron. J. Mol. Des. **2009**, 8 (2), 14–28

Abstract

Motivation. The quest for design of selective nontoxic anti–inflammatory analgesic agent is continuously going on since more than last 30 years. Keeping the same objective in mind as an attempt to develop potent and nontoxic, nonsteroidal analgesic anti–inflammatory agents, we have optimized the diaryl pharmacophore by using molecular modeling studies.

Method. In this paper we present results of 2D and 3D QSAR studies of series of 80 molecules containing 4,5–diarylimidazole pharmacophore as selective cyclooxygenase–2 (COX–2) inhibitors. The 3D QSAR studies were performed using two different methods, stepwise variable selection *k*–nearest neighbor molecular field analysis (SW kNN–MFA) and simulated annealing *k*–nearest neighbor molecular field analysis (SA kNN–MFA) methods. The 2D QSAR studies were performed using multiple regression.

Results. 3D QSAR studies produced reasonably good predictive models with high cross–validated r^2_{cv} value of 0.688 and 0.733 and conventional r^2 value of 0.912 and 0.794 values using the models SW kNN–MFA and SA kNN–MFA method respectively, whereas the r^2 value in 2D QSAR studies was found to be 0.8943.

Conclusions. The output of present research work is interesting, the 2D QSAR studies indicated contribution of different physicochemical descriptors and the result of 3D QSAR studies indicated the exact steric and electronic requirement in the ranges at various positions around 4,5–diaryl imidazole pharmacophore. Thus the pharmacophore requirement for selective COX–2 inhibition was optimized and requirement at various positions around 4,5–diaryl imidazole pharmacophore were defined.

Keywords. Cyclooxygenase–2; COX–2; diaryl imidazole; 3D QSAR; molecular field analysis.

1 INTRODUCTION

The market for NSAIDs is expanding rapidly because of an ageing population in developed countries and the associated increase in the prevalence of diseases like arthritis. Use of aspirin is also increasing because of its utility in reducing the incidences of number of common disorders including stroke, myocardial infraction, Alzheimer's disease and cancer [1]. In the recent years,

* Correspondence author; phone: 91–20–26058204; fax: 91–20–26058208; E–mail: drugdesign1@gmail.com.

several novel approaches for reducing the GI toxicity of NSAIDs with promising results have been reported [2].These mainly involve structural modifications of existing NSAIDs such that inhibition of COX is maintained, but other attributes are added that diminish GI (and other) toxicity and in some cases boost efficacy and/or potency [3]. In 1997,it was found that about 5– 6 % of world population in many regions is suffering from rheumatoid arthritis (RA) while osteoarthritis (OA) was claimed to affect about 10% of the world's population of which 50% were the elderly population [4,5]. The expression of COX–2 in brain, kidney and bone marrow has made it an attractive therapeutic target for designing selective drugs for Alzheimer's disease, cancer etc. The efficacy of these drugs is proven to be better than that of traditional NSAIDs, with no or little side effects associated with traditional NSAIDs [6]. More than 100 related metabolic products derived from arachidonic acid and synthesized by cyclooxygenase (COX). Prostaglandin play broad role in normal human physiology; it is not surprising that systematic suppression of PG synthesis through inhibition of COX can lead to unwanted side effects. The rate limiting step in the synthesis of prostaglandins and thromboxane is the conversion of arachidonate to prostaglandin H_2, which is catalyzed by cyclooxygenase enzymes. COX exists in two different isoforms namely, COX–1 and COX–2 [7]. It was subsequently determined that the COX–1 and COX–2 protein are derived from distinct genes [8,9]. The expression and physiological functions of two isoforms are also different [10]. As many as 25% of individuals consuming NSAIDs experience some type of side effects and as many as 5% developed serious health consequences [11,12]. Selective inhibition of this COX–2 enzyme overcomes gastrointestinal (GI) side effects associated with traditional NSAIDs.

Non steroidal anti–inflammatory drugs (NSAIDs) are widely used for the treatment of pain and inflammation especially arthritis, arthritis–associated disorders [13]. Following the discovery of the inducible isozyme cyclooxygenase –2 in 1991 and with the advent of several selective COX–2 inhibitors, still selective inhibition of COX–2 over COX–1 continued to be an attractive target for anti inflammatory therapy. Some of the selective COX–2 inhibitors with proven therapeutic utility for the treatment of inflammation include Celecoxib [14], Rofecoxib [15], Valdecoxib [16] and Etoricoxib [17]. The major goal of this work is to optimized substituent's on to the 4, 5–diarylimidazole pharmacophore, in order to increase selective inhibition of COX–2 and in turn enhance anti–inflammatory activity by using 3–D QSAR studies and with the aim of designing compounds with a wider margin of safety, especially with reference to the Gastrointestinal ulcerogenicity.

2 MATERIALS AND METHODS

2.1 Biological Data

Eighty molecules, reported for their COX–2 effect [18] were selected for the present study. The structures of the compounds and their biological data are presented in Table 1. In order to correlate

the free energy changes during in vivo interactions of reported compounds with the target enzyme, the ED_{50} values were converted to pED_{50}:

$$pED_{50} = -\log ED_{50} \quad (1)$$

All computational studies were performed using V–Life Molecular Design Software Version 3.0 [19]. Both 2D and 3D QSAR models were generated using a training set of 70 molecules. Test set of 10 molecules with distributed biological were used to access the predictive power of generated QSAR models using training set of 70 molecules with varied chemical and biological activities. In addition, the molecules in the test set should be selected in such a way that there lie few similarities with the compounds in training set. For example the variation in structural composition, biological activity ranges etc.

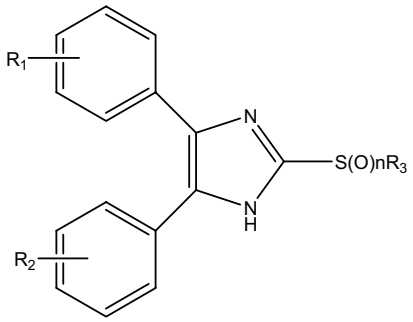

Figure 1. Common template for 4, 5–diaryl imidazole series.

Table 1. The selected series of 4, 5–diaryl imidazole along with their biological activity data

Mol	n	R_1	R_2	R_3	ED_{50}	$1/ED_{50}$	$\log 1/ED_{50}$
1	0	–H	–H	$-CH_3$	100	0.01	–2
2	0	–4–F	–4–F	$-CH_3$	4	0.25	–0.6
3	0	–4–Cl	–4–Cl	$-CH_3$	4	0.25	–0.6
4	0	–4–F	–4–Cl	$-CH_3$	3.8	0.2631	–0.5799
5	0	$-4-OCH_3$	$-4-OCH_3$	$-CH_3$	4.5	0.22	–0.6576
6	0	$-4-OCH_3$	$-4-OCH_3$	$-CH_3$	25	0.04	–1.3979
7	0	$-4-CH_3$	$-4-CH_3$	$-CH_3$	25	0.04	–1.3979
8	0	$-4-CF_3$	$-4-CF_3$	$-CH_3$	9	0.11	–0.9586
9	0	$-4-CF_3$	$-4-CF_3$	$-CH_3$	9	0.11	–0.9586
10	0	$-4-CF_3$	$-4-CF_3$	$-CH_3$	17	0.065	–1.1871
11	0	$-4-CF_3$	$-4-CF_3$	$-CH_3$	3.6	0.3	–0.5229
12	0	–3–F	–3–F	$-CH_3$	75	0.013	–1.8861
13	0	–3–Cl	–3–Cl	$-CH_3$	50	0.02	–1.699
14	0	–H	–H	$-C_2H_5$	100	0.01	–2
15	0	$-4-OCH_3$	$-4-0CH_3$	$-C_2H_5$	5	0.2	–0.699
16	0	$-4-OCH_3$	$-4-OCH_3$	$-CH=CH_2$	12	0.083	–1.081
17	0	$-4-OCH_3$	$-4-OCH_3$	–n–propyl	9	0.11	–0.9586
18	0	$-4-OCH_3$	$-4-OCH_3$	–Allyl	20	0.05	–1.301
19	0	–H	–3,4–diCl	$-CH_3$	25	0.04	–1.3979
20	0	$-4-OCH_3$	$-4-OCH_3$	–Isoprpyl	30	0.03	–1.5229
21	0	–H	–H	–n–Butyl	75	0.013	–1.8861
22	0	–H	–H	$-CH_2CF_3$	150	0.0067	–2.1739
23	0	–4–Cl	–4–Cl	$-CH_2CF_3$	4	0.25	–0.6
24	0	$-4-OCH_3$	$-4-OCH_3$	$-CH_2CF_3$	35	0.029	–1.5376
25	0	–H	–H	$-CH_2CF_2CF_3$	70	0.014	–1.8539
26	0	$-4-OCH_3$	$-4-OCH_3$	$-CH_2COCH_3$	10	0.1	–1
27	0	–H	$-4-OCH_3$	$-CH_2-S-CH_3$	50	0.02	–0.1699

Table 1. (Continued)

Mol	n	R_1	R_2	R_3	ED_{50}	$1/ED_{50}$	log $1/ED_{50}$
28	0	–4–OCH_3	–4–OCH_3	–CH_2–S–CH_3	30	0.03	–1.5229
29	0	–4–OCH_3	–4–OCH_3	–CH_2–SO–CH_3	52	0.019	–1.7212
30	0	–H	–H	–CH_3	100	0.01	–2
31	1	–4–F	–4–F	–CH_3	4	0.25	–0.6
32	1	–4–Cl	–4–Cl	–CH_3	2.5	0.04	–1.3979
33	1	–4–OCH_3	–4–OCH_3	–CH_3	6.5	0.154	–0.8125
34	1	–H	–3–F	–CH_3	100	0.01	–2
35	1	–H	–Cl	–CH_3	75	0.013	–1.8861
36	1	–H	–3,4–diCl	–CH_3	50	0.02	–1.699
37	1	–H	–H	–C_2H_5	75	0.013	–1.8861
38	1	–4–OCH_3	–4–OCH_3	–C_2H_5	10	0.1	–1
39	1	–4–OCH_3	–4–OCH_3	–n–propyl	15	0.067	–1.1739
40	1	–4–OCH_3	–4–OCH_3	–Isopropyl	30	0.03	–1.5229
41	1	–H	–H	–n–Butyl	100	0.01	–2
42	1	–H	–H	–CH_2–CF_3	75	0.013	–1.8861
43	1	–4–Cl	–4–Cl	–CH_2–CF_3	2.3	0.4347	–0.3618
44	1	–4–OCH_3	–4–OCH_3	–CH_2–CF_3	11	0.091	–1.041
45	1	–H	–H	–CH_2–CH_2–CF_3	75	0.013	–1.8861
46	1	–H	–H	–CH_2–CF_2–CF_2	75	0.013	–1.8861
47	1	–H	–H	–CH_2–CH_2–CF_2–CF_3	75	0.013	–1.8861
48	1	–4–OCH_3	–4–OCH_3	–CH_2–S–CH_3	28	0.035	–1.4559
49	1	–4–F	–4–F	–CH_3	4.5	0.22	–0.6576
50	2	–4–OCH_3	–4–OCH_3	–CH_2–$COCH_3$	35	0.029	–1.5376
51	1	–4–Cl	–4–Cl	–CH_3	2	0.5	–0.301
52	2	–H	–4–F	–CH_3	9	0.11	–0.9586
53	2	–H	–4–Cl	–CH_3	30	0.03	–1.5229
54	2	–4–F	–4–Cl	–CH_3	2.8	0.36	–0.4437
55	2	–4–OCH3	–4–0CH_3	–CH_3	10	0.1	–1
56	2	–H	–4–OCH_3	–CH_3	25	0.04	–1.3979
57	2	–H	–4–OC_2H_5	–CH_3	50	0.02	–1.699
58	2	–H	–4–CH_3	–CH_3	100	0	0
59	2	–H	–4–CF_3	–CH_3	50	0.02	–1.699
60	2	–4–F	–4–CF_3	–CH_3	3.7	0.27	–0.5686
61	2	–4–Cl	–4–CF_3	–CH_3	2.2	0.45	–0.3468
62	2	–2–Cl	–3–Cl	–CH_3	50	0.02	–1.699
63	2	–H	–3–F	–CH_3	75	0.013	–1.8861
64	2	–H	–3–Cl	–CH_3	10	0.01	–1
65	2	–H	–3,4–diCl	–CH_3	50	0.02	–1.699
66	2	–H	–H	–CH_2–CH_3	100	0.01	–2
67	2	–4–OCH_3	–4–O–CH_3	–CH_2–CH_3	6	0.17	–0.7696
68	2	–H	–H	–n–Propyl	100	0.01	–2
69	2	–4–OCH_3	–4–O–CH_3	–n–propyl	9.5	0.11	–0.9586
70	2	–4–OCH_3	–4–OCH_3	–Allyl	10	0.1	–1
71	2	–4–OCH_3	–4–OCH_3	–Isopropyl	30	0.03	–1.5229
72	2	–H	–H	–n–Butyl	100	0.01	–2
73	2	–H	–H	–CH_2–CF_3	50	0.02	–1.699
74	2	–4–F	–4–F	–CH_2–CF_3	3.5	0.29	–0.5376
75	2	–4–Cl	–4–Cl	–CH_2–CF_3	10	0.1	–1
76	2	–4–OCH_3	–4–OCH_3	–CH_2–CF_3	75	0.013	–1.8861
77	2	–H	–H	–CH_2–CF_2–CF_3	75	0.013	–1.8861
78	2	–H	–H	—CH_2–CF_2–CF_3	100	0.01	–2
79	2	–H	–H	–CH_2–CH_2—CF_2–CF_3	75	0.013	–1.8861
80	2	–4–OCH_3	–4–OCH_3	–CH_2–$COCH_3$	20	0.05	–1.301

Additional care was taken while selecting compounds in training and test set, that all these compounds retain similarity in chemical composition with respect to mode and locus of binding at

active binding binding pocket of COX–2 enzyme. The goal was to ensures the accuracy of predictive abilities of models developed.

2.2 2D–QSAR Studies

The use of quantitative structure activity relationship since its advent [20] has become increasingly helpful in understanding many aspects of chemical–biological interactions of drug and pesticide research as well as many areas of toxicology. The COX–2 inhibitory data have been collected from the literature. It is expressed as ED_{50}, the molar concentration of the compounds causing 50% inhibition of the COX–2. The negative algorithm of IC_{50} (pIC_{50}) was used as biological activity in the 3D QSAR study thus corelating the data linear to the free energy change. The initial conformations were obtained from systematic search. The lowest energy conformers were selected and minimized until root–mean–square (RMSD) of 0.001 kcal/mol Å was achieved. All the physicochemical properties are auto loaded and the QSAR regression analysis were executed with V–life Molecular Design Suite Software. The most widely used Multiple Linear regression (MLR) analysis was used to correlate biological activities with physicochemical properties in turn chemical composition of selected series of compounds.

2.3 3D QSAR Studies using kNN MFA [21]

The compounds were constructed from the fragments in the V–Life molecular builder database with standard bond lengths and bond angles and geometry optimization was carried out using the standard Merck molecular force field (MMFF) [22] with distance dependant –dielectric function and energy gradient of 0.001 kcal/mol Å. The template used for alignment is shown in (figure 2). Alignment of compounds is a very important feature for developing kNN MFA analysis. For each alignment, the steric and electrostatic potential fields for KNN MFA were calculated at each lattice intersection of a regularly spaced grid box. The lattice spacing was set to value of 2.0 Å in all *X*, *Y* and *Z* directions. A distance–dependant dielectric constant of 1.0 was used. An sp^3 carbon atom with van der Waals radius of 1.52 Å and + 1.0 charge was served as the probe atom to calculate steric and electrostatic fields (Figure 3). All 70 molecules in the training set were considered as observation to generate QSAR equations using Simulated Annealing (SA) and stepwise (SW) kNN MFA methods.

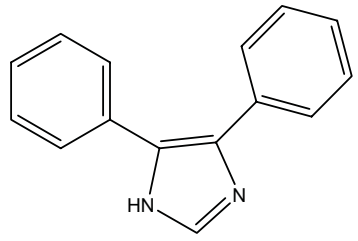

Figure 2. Common template used for alignment of 4, 5–diaryl imidazole series of compounds.

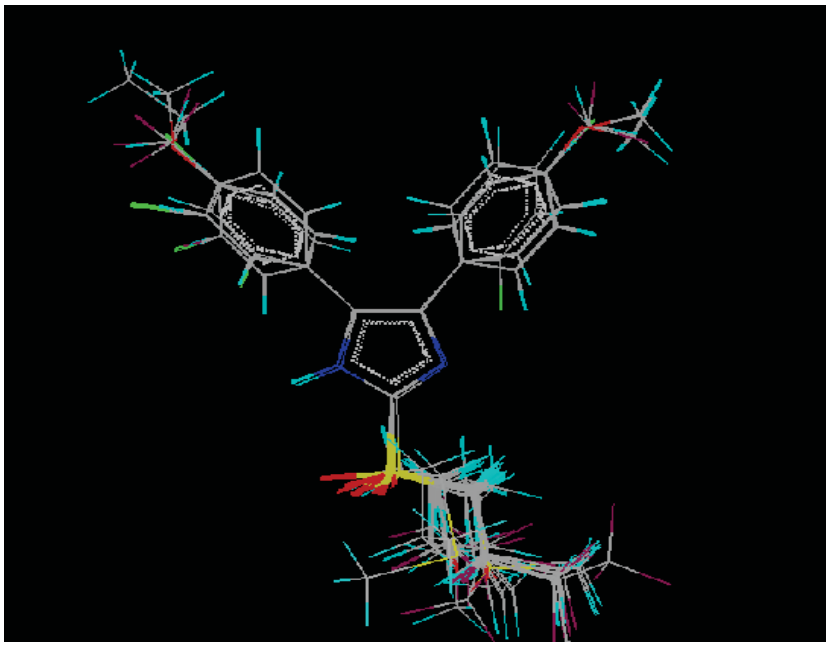

Figure 3. Superposition of all molecules of 4,5–diaryl imidazole series of compounds aligned with V–Life MDS.

3 RESULTS AND DISCUSSION

3.1 2D–QSAR studies

2D QSAR Studies were performed using VLife Molecular Design Suite software. 2D QSAR Equation was generated using multiple linear regression. The preliminary information obtained from 2D QSAR analysis was used while defining nature of substituent's when the NCEs were designed and their biological activity was predicted. The QSAR model is presented as Eq. (2):

$$pIC_{50} = -10.685 + 0.673\times XlogP - 0.457\times slogP + 49.216\times xk\_Avg.Hydrophobocity + 3.190\times DistTopo - 0.117\times smr + 1.173\times chiV0 - 0.561\times k1alpha) - 0.004\times vdWSurfaceArea + 50.125\times Average–vePotential + 4.366\times IdAverage - 4.857\times SAAverage \quad (2)$$

The relative contribution of each descriptor for the biological activity as selective COX–2 inhibitors is presented in (Table 2).

Table 2. Results of 2D–QSAR equation obtained by Multiple Linear Regression Equation.

Sr. No	Statistical Parameters	Results	Positively Contributing Descriptors	Negatively Contributing Descriptors
1	$r^2CV(q^2)$	0.749149		
2	r^2	0.8943	1. XlogP	
3	r	0.9457	2.xkAvg.Hydrophobicity	1. slogp
4	SEE	0.370280	3. Dist. Topo.	2. smr
5	F–Test	12.239766	4. Avg.–vePotential	3. SAAverage
6	Alpha	0.0016	5. IdAverage	4. k1alpha
7	Best–Ran_q^2	0.2356	6. chiV0	5. vdW Surface Area
8	Zscore	9.8213		

The regression equation indicated that the positively contributing descriptors were directly proportions to the biological activity, increasing of these properties in the molecules will increases Cox–2 activity. Where as negative correlated descriptors were inversely proportion to COX–2

activity and it was required to decrease these properties in the compound for better Cox–2 activity.

XlogP signifies ratio of solute concentration in octanol and water and generally termed as octanol water partition coefficient. This was atom based evaluation of logP and positive correlation indicated that molecules with higher ratio is significant for better activity where as negative correlation of slogp showed that compound with less protonation state were increases the activity as this descriptor signifies log of the octanol/water partition coefficient (including implicit hydrogens) which is an atomic contribution model that calculates logP from the given structure; i.e., the correct protonation state. Similarly positive contribution of XKAverageHydrophobicity, DistTopo, Average–vePotential, IdAverage, chiV0 indicated that hydrophobicity on van der Waals surface, topological index; average of total negative electrostatic potential will be increases for better biological activity.

3.2 3D QSAR Studies

3D QSAR Studies were performed using V Life Molecular Design Suite software. For generation of 3D QSAR model, k Nearest Neighbor Molecular Field Analysis (kNN MFA) method was used in conjunction with Simulated Annealing (SA) and Stepwise (SW) variable selection method and alignment of the molecules was carried out using Template based alignment. The training set of molecules comprised compounds with varying chemical nature and exhibiting a wide range (minimum pIC_{50} = –2.174, maximum pIC_{50} = –0.347) of biological activity were selected so that they provide critical information on pharmacophore requirements. Predictive power of resulting models was evaluated using test set of ten molecules. Selection of test set molecule was made by considering the fact that biological activity of test set was widely distributed and within the range of training set. Both models were developed using same training and test set of molecules. The statistical results of SA and SW kNN–MFA model are summarized in Table 3.

Table 3. Summary of sStatistical sesults of kNN MFA models for 4, 5–diaryl imidazole series of COX–2 inhibitors.

Sr. No.	PARAMETERS	SA kNN–MFA	SW kNN–MFA
1	opt_q^2	0.733	0.688
2	opt_pred_r^2	0.794	0.912
3	Z score_q^2	8.951	6.151
4	best_ran_q^2	–0.04111	–0.16395
5	Alpha	0	1.35E–08
6	K	5	3
Contributing Descriptors			
	Contributing Steric parameters	STE291,(–0.2083,0.073) STE829,(17.841,30.00) STE1097.(30.00,30.00)	STE 552,(–0.4492,–0.4465) STE 746,(–0.1083,–0.1062) STE 829,(30.00,30.00) STE 974.(–0.1802,0.3283)
	Contributing Electronic parameters	ELE186, (–0.0475,0.221) ELE460,(5.088,10.00) ELE590,(2.5342,10.00) ELE982,(–10.00,–10.00) ELE1217.(–0.4449,0.615)	ELE 187,(–0.253,0.0708) ELE 460,(2.5342,3.1114) ELE 1136, (–0.595,–0.503) ELE 1240,(–3.0420,1.430) ELE 1252,(–0.7252,–0.133) ELE 1358.(–2.097,1.5595)

All the statistical results, cross–validation were analyzed by considering the fact that a value of cross–validated r^2 (r^2_{cv}) is above 0.5 indicating the probability of getting correlation value by chance is less than 5%. The statistical results obtained by both SA and SW kNN–MFA studies (Table 3).

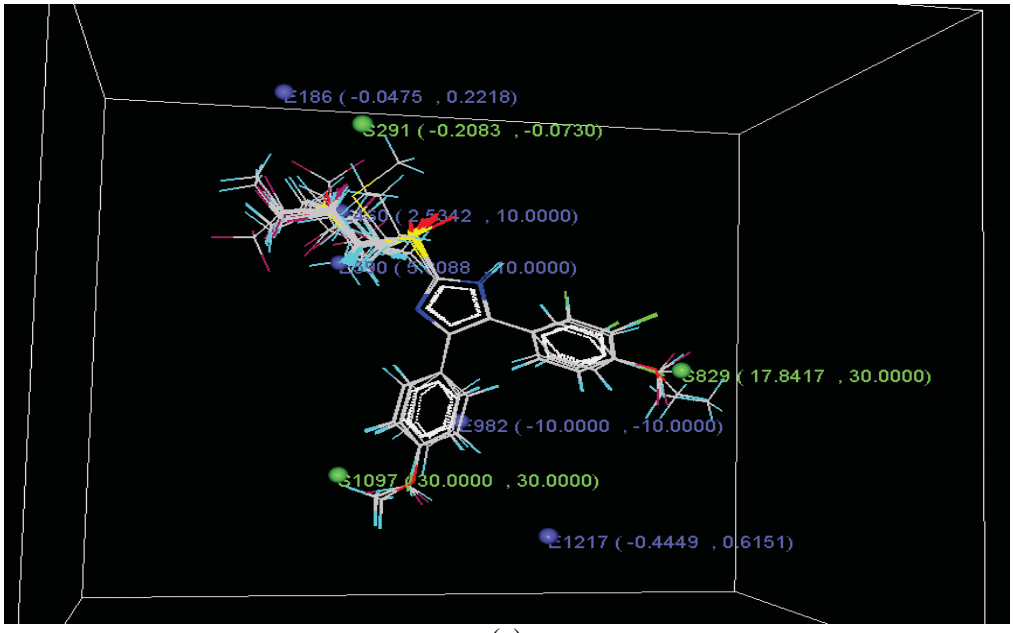

(*a*)

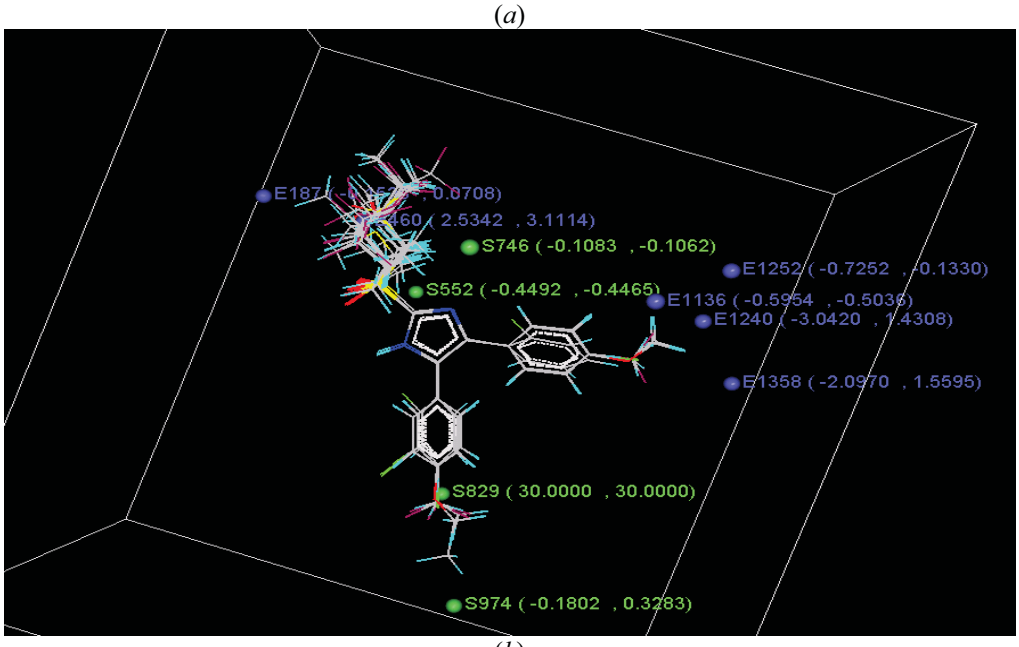

(*b*)

Figure 4. Stereo view of the molecular rectangular field grid around the superposed molecular units of 4,5 diaryl imidazole series using SA (*a*) and SW (*b*) kNN MFA Methods respectively.

Simulated Annealing k–Nearest Neighbor Molecular Field Analysis (SA KNN MFA)

Several 3D QSAR model were generated using SA kNN–MFA method with 80 compounds and best model were reported here, yielded a q^2 (r^2_{cv}) of 0.733 and a conventional correlation coefficient (r^2) of 0.794. The predictive ability of this MFA Model was evaluated by predicting the biological

activities of the test set molecules.

The various results for statistical analysis worth mentioning are the Z–score = 8.951 which ideally should be as high as possible, best randomized q^2 = –0.04111 which ideally should be as low as possible. The stereo view of the molecules selected for 3D QSAR studies with a generated rectangular field grid is shown in (Figure 4). The relative contributions of steric and electrostatic parameters were 62.50% and 37.50% for SA kNN MFA model. Close analysis indicated that the statistical results obtained are nearer to the ideal requirement, therefore it can be concluded that the resultant QSAR model has very good predictive ability and will be used for optimizing the pharmacophore requirement of 4,5–diarylimidazole for better COX–2 activity.

Stepwise k–nearest neighbor Molecular Field Analysis Method (SW kNN MFA Method)

Several 3D QSAR model were generated using SW kNN MFA method and best model with 80 compounds were reported here, yielded an r^2_{cv} of 0.688 and a conventional correlation coefficient (r^2) of 0.912. The predictive ability of this MFA model was evaluated by predicting the biological activities of test set molecules and best model was selected on the basis of error occurred in the predicting ability of the model (q^2_SE, pred_r^2_SE). Stereo view of the molecular rectangular field grid around the superposed molecular units of 4,5–diaryl imidazole series using SW kNN MFA methods, are shown in Figure 4. The relative contributions of steric and electrostatic parameters were 40% and 60% For SW kNN MFA model. The tabular and graphical representation of actual, predicted activities and the residuals there of (actual pIC_{50} minus predicted activities) for the training set and test set molecules using both SA and SW kNN MFA method are presented in Table 4 and 5 respectively, and Figure 5 and 6 respectively.

Table 4. Training set of COX–2 inhibitors from 4,5–diaryl imidazole series along with biological activities and predicted activity and residual of observed activity minus predicted activity

No.	Mol.	pIC_{50}	SA–kNNMFA		SW–kNNMFA	
			Computed	Residual	Computed	Residual
1	1.mol2	–2.000	–1.969	–0.031	–1.955	–0.045
2	2.mol2	–0.600	–1.044	0.444	–1.078	0.478
3	5.mol2	–0.658	–1.023	0.366	–1.185	0.527
4	6.mol2	–1.398	–1.165	–0.233	–1.277	–0.121
5	7.mol2	–1.398	–1.073	–0.325	–1.270	–0.128
6	8.mol2	–0.959	–0.538	–0.421	–0.703	–0.256
7	9.mol2	–0.959	–1.512	0.553	–1.345	0.387
8	10.mol2	–1.187	–0.870	–0.317	–0.733	–0.454
9	12.mol2	–1.886	–1.809	–0.077	–1.961	0.074
10	14.mol2	–1.398	–1.161	–0.237	–1.298	–0.100
11	15.mol2	–2.000	–1.969	–0.031	–1.955	–0.045
12	16.mol2	–0.699	–1.159	0.460	–1.163	0.464
13	17.mol2	–1.081	–1.155	0.074	–1.092	0.011
14	18.mol2	–0.959	–0.932	–0.026	–1.039	0.081
15	19.mol2	–1.301	–0.954	–0.347	–0.984	–0.317
16	20.mol2	–1.523	–0.962	–0.561	–1.056	–0.466
17	21.mol2	–1.886	–2.000	0.114	–1.977	0.090
18	22.mol2	–2.174	–1.801	–0.373	–1.796	–0.378

Table 4. (Continued)

No.	Mol.	pIC_{50}	SA–kNNMFA		SW–kNNMFA	
			Computed	Residual	Computed	Residual
19	23.mol2	–0.600	–0.726	0.126	–0.757	0.157
20	24.mol2	–1.538	–1.670	0.132	–1.337	–0.200
21	25.mol2	–1.854	–1.826	–0.028	–1.969	0.115
22	26.mol2	–1.000	–0.758	–0.242	–0.521	–0.479
23	27.mol2	–1.699	–1.957	0.258	–1.932	0.233
24	28.mol2	–1.523	–1.672	0.150	–1.483	–0.04
25	29.mol2	–1.721	–1.620	–0.101	–1.698	–0.023
26	30.mol2	–2.000	–1.898	–0.102	–1.924	–0.076
27	31.mol2	–0.600	–0.969	0.369	–1.058	0.458
28	32.mol2	–1.398	–0.975	–0.423	–0.771	–0.627
29	33.mol2	–0.813	–1.109	0.296	–1.326	0.513
30	35.mol2	–1.886	–1.429	–0.458	–1.491	–0.395
31	36.mol2	–1.699	–1.529	–0.170	–1.601	–0.098
32	37.mol2	–1.886	–1.950	0.064	–1.977	0.091
33	38.mol2	–1.000	–1.064	0.064	–1.274	0.274
34	39.mol2	–1.174	–1.432	0.258	–1.114	–0.060
35	40.mol2	–1.523	–0.937	–0.585	–1.074	–0.448
36	41.mol2	–2.000	–1.927	–0.073	–1.922	–0.078
37	42.mol2	–1.886	–1.917	0.031	–1.923	0.036
38	43.mol2	–0.362	–0.494	0.132	–0.419	0.057
39	44.mol2	–1.041	–0.930	–0.111	–1.028	–0.013
40	45.mol2	–1.886	–1.950	0.064	–1.923	0.037
41	46.mol2	–1.886	–1.916	0.030	–1.939	0.053
42	47.mol2	–1.886	–1.956	0.069	–1.963	0.076
43	48.mol2	–1.538	–1.619	0.082	–1.648	0.110
44	49.mol2	–1.456	–1.157	–0.299	–1.066	–0.390
45	50.mol2	–0.658	–0.403	–0.255	–0.479	–0.179
46	51.mol2	–0.301	–0.518	0.217	–0.454	0.153
47	52.mol2	–0.959	–1.547	0.589	–1.662	0.703
48	55.mol2	–1.000	–1.083	0.083	–0.993	–0.007
49	56.mol2	–1.398	–1.584	0.187	–1.519	0.121
50	57.mol2	–1.699	–1.520	–0.179	–1.416	–0.283
51	58.mol2	–2.000	–1.760	0.240	–1.805	0.195
52	59.mol2	–1.699	–1.518	–0.181	–1.413	–0.286
53	61.mol2	–0.347	–0.526	0.179	–0.443	0.096
54	62.mol2	–1.699	–1.630	–0.069	–1.542	–0.157
55	63.mol2	–1.886	–1.494	–0.393	–1.351	–0.535
56	65.mol2	–1.699	–1.541	–0.158	–1.518	–0.181
57	66.mol2	–2.000	–1.931	–0.069	–1.922	–0.078
58	67.mol2	–0.770	–0.956	0.186	–1.186	0.416
59	68.mol2	–2.000	–1.897	–0.103	–1.931	–0.069
60	69.mol2	–0.959	–0.720	–0.239	–0.472	–0.487
61	70.mol2	–1.000	–1.123	0.123	–1.289	0.289
62	71.mol2	–0.523	–0.835	0.312	–0.670	0.147
63	72.mol2	–2.000	–1.972	–0.028	–1.962	–0.038
64	73.mol2	–1.699	–1.966	0.267	–1.935	0.236
65	74.mol2	–0.538	–0.731	0.193	–0.818	0.280
66	75.mol2	–1.000	–0.550	–0.450	–0.554	–0.446
67	76.mol2	–1.886	–1.564	–0.322	–1.610	–0.277
68	77.mol2	–1.886	–1.931	0.045	–1.920	0.034
69	78.mol2	–2.000	–1.846	–0.154	–1.804	–0.196
70	79.mol2	–1.886	–1.902	0.016	–1.961	0.075

Table 5. Test set of COX–2 inhibitors from 4,5–diaryl imidazole series along with biological activities and predicted activity and residual of observed activity minus predicted activity

No.	Mol.	pIC_{50}	SA–kNNMFA		SW–kNNMFA	
			Computed	Residual	Computed	Residual
1	3.mol2	–0.600	–0.959	0.359	–0.593	–0.007
2	4.mol2	–0.580	–0.960	0.380	–0.607	0.027
3	11.mol2	–0.523	–0.923	0.400	–0.801	0.278
4	13.mol2	–1.699	–1.886	0.187	–1.914	0.215
5	34.mol2	–2.000	–1.826	–0.174	–1.791	–0.209
6	53.mol2	–1.523	–1.519	–0.004	–1.506	–0.017
7	54.mol2	–0.444	–0.394	–0.049	–0.412	–0.031
8	60.mol2	–0.569	–0.461	–0.108	–0.602	0.033
9	64.mol2	–1.000	–1.567	0.567	–1.431	0.431
10	80.mol2	–1.301	–1.613	0.312	–1.669	0.368

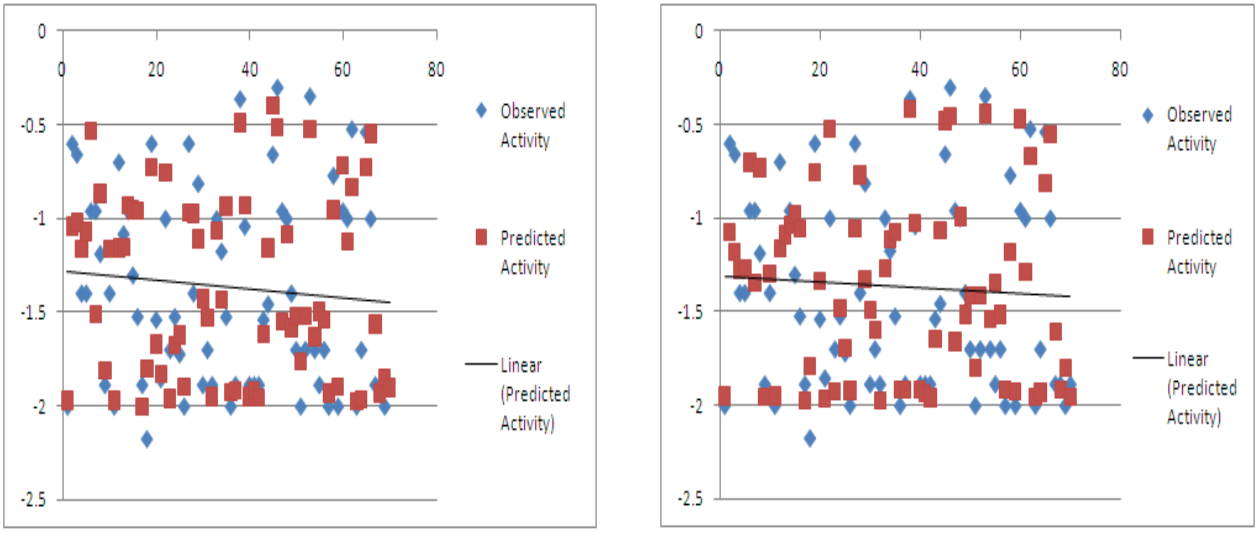

(*a*) (*b*)

Figure 5. Plot of observed activity vs predicted activity for training set of 4,5–diaryl imidazole series of compounds using SA kNN MFA (*a*) and SW kNN MFA (*b*) methods, respectively.

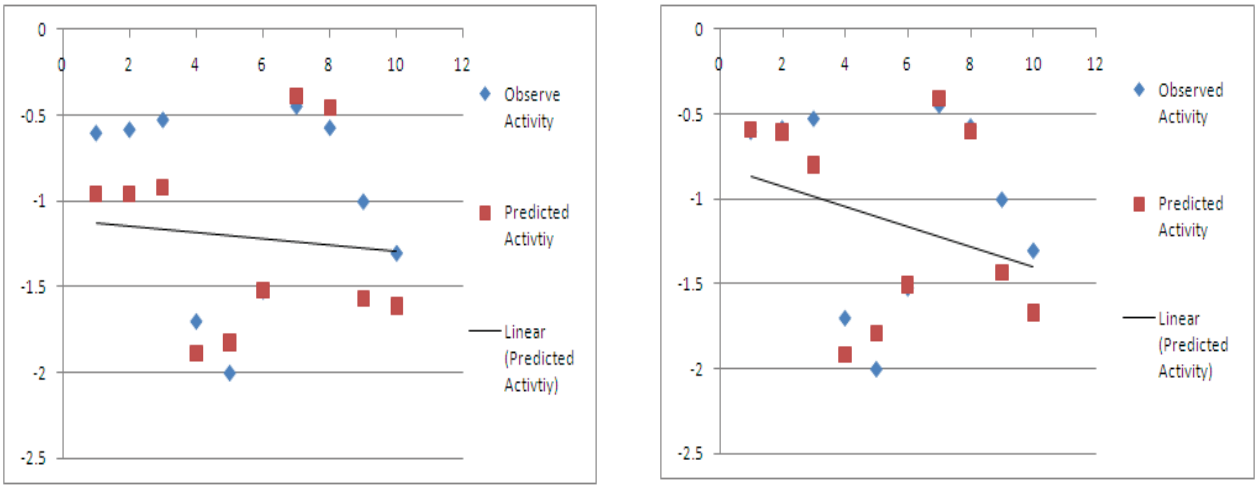

(*a*) (*b*)

Figure 6. Plot of observed activity vs predicted activity for test set of 4,5–diaryl imidazole series of compounds using SA kNN MFA (*a*) and SW kNN MFA (*b*) methods, respectively.

Tables 3 and 4 showed residual obtained by subtraction of predicted activities from biological activities in both model was low, thus error occurred in prediction of biological activity by both model is near to zero which indicated power of predicating the biological activity is good. Thus both SA and SW kNN MFA model will be used for deigned of new potent compounds containing 4,5–diaryl imidazole nucleus for selective inhibition of COX–2 enzyme.

3.3 Optimization of Pharmacophore

The information obtained from 3D and 2D QSAR studies was used to optimize the electrostatic and steric requirement around the 4,5–diaryl imidazole nucleus for selective inhibition of COX–2 (Figure 7).

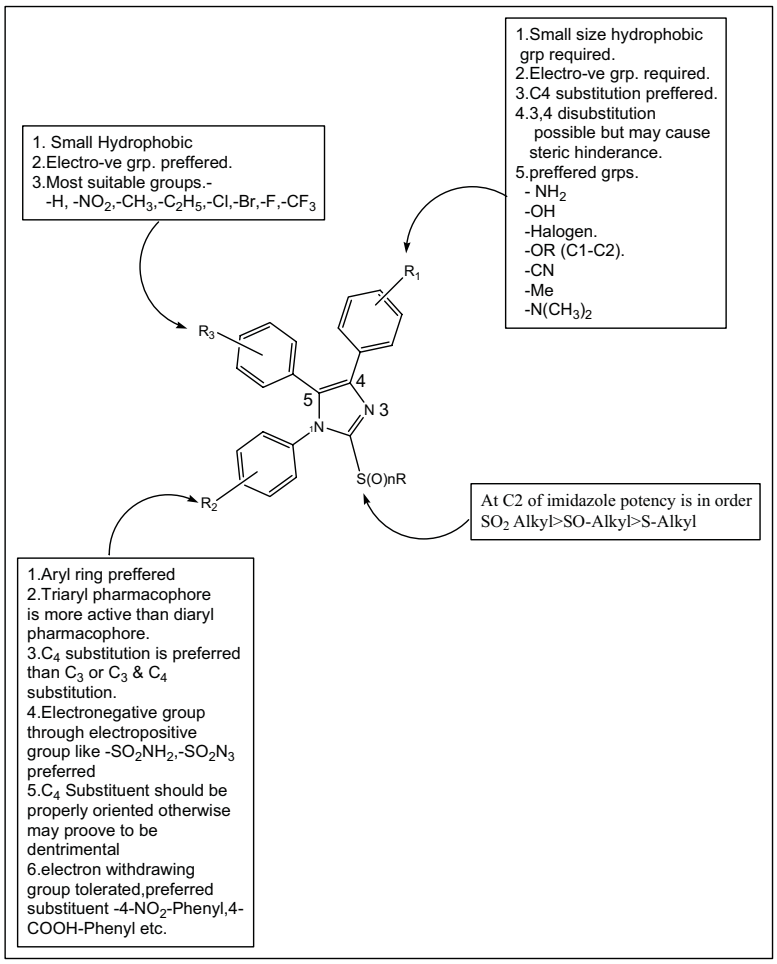

Figure 7. Requirements around 4,5–triaryl imidazole pharmacophore for selective inhibition of COX–2.

The relevant findings of present work are summarized below.

1. C_2 of Imidazole Ring

A. Electrostatic interactions. The close inspection of 3D data points generated by both KNN MFA models indicates that a small size electropositive group like S–alkyl, SO–alkyl, SO_2–alkyl are tolerated at C_2 of 4,5–diaryl imidazole pharmacophore through electropositive atoms like S, as SO_2

contribute significantly for COX–2 inhibitory activity. The electrostatic data points (positive range) shown in (Figure 1) around C_2 of 4,5–diaryl imidazole indicates requirement of electropositive groups for selective COX–2 inhibitory activity.

B. **Steric Interactions.** Since the steric data points generated around C_2 substituent of 4,5–diaryl imidazole pharmacophore indicates small negative ranges, it can be said that large bulky groups are not favored on the electropositive S atom at C_2 of imidazole. Small alkyl groups substituted through S may be favorable. The compounds containing S atom with 2 oxygen functions at C_2 of 4,5–diaryl imidazole pharmacophore are more potent thus only S atom containing compounds interactions with COX–2 enzymes. The same pattern can be observed with pattern of predicted activities for test set of compounds, probably due to the reason that more electropositive atom is required at C_2 of imidazole ring.

2. 4–Phenyl Substitution Pattern

A. Electrostatic interactions. The SA kNN MFA model did not predict the electrostatic data points as far as substitution pattern around C_4 phenyl ring is concerned. But the SW kNN MFA model shows very informative electrostatic data points. All electronic data point ranges are indicating negative values at 4^{th} position of C_4.Phenyl ring suggesting requirement of electronegative groups like $–NH_2$,–OH,–Halogen, Alkoxy, nitrile, alkyl, alkyl, and amino groups substituted at Para position of C4 phenyl ring. No data points were generated at or around any other position of phenyl ring since substitution pattern were restricted to 4^{th} position of C4 phenyl in all the selected training set compounds for 3D QSAR studies.

B. Steric interaction. Since only one 3D steric data point was generated in SA model indicating negative range and none in SW model indicates requirements of small hydrophobic bulk at/Para position of C4 phenyl ring. Looking at results of predicted activities it can be said that most preferred substituent at para position of C4 phenyl ring is small electronegative functional groups such as $–NH_2$, –OH, $–CH_3$, $–OCH_3$, $–OC_2H_5$, etc.

3. C5 Phenyl Substitution Pattern

Both SA and SW kNN MFA models show only steric 3D data points at/around 4^{th} position of C5 phenyl ring of 4,5 diaryl imidazole pharmacophore .the value for these steric data points are high and towards positive sites, suggesting the requirements of bulky/hydrophobic substituent's at 4^{th} position of C5 phenyl ring. Close analysis of results indicates the requirements of moderately bulkier but hydrophobic groups at 4^{th} position of C5 phenyl ring. Additional increase in bulk at 4^{th} position of C5 phenyl may deleterious as it would probably create steric hindrance for selective binding of COX–2 active site. In all it can be said that results obtained by 3D KNN MFA studies by SA and SW methods are complimentary to each other and are in agreement with the reported results of general requirements of selective and ideal pharmacophore for selective COX–2 binding and in

turn inhibition.

4 CONCLUSIONS

The thorough investigation of result of 2D and 3D QSAR studies have helped us to decide about the electronic and steric nature of substitution pattern around the selected 4,5–diaryl imidazole nucleus. At various positions on the common template the substitution pattern was carried out and the same data was used for the design of NCEs. The regression equation obtained was used for prediction of activity of designed compounds in silico. In all the overall outcomes of these studies have provided great help to optimize the pharmacophore and to design the potent, selective COX–2 inhibitors compounds.

5 REFERENCES

[1] A. Burger, Burgers Medicinal Chemistry and Drug Discovery, John WILY and Sons, Inc., NewYork; 5th Edition **1995**, 3–4.
[2] K. D. Rainsford, The ever–emerging anti–inflammatories. Have there been any real advances, *J. Physiol. Paris* **2001**, *95*, 11–19.
[3] R. W. Dubois, G. Y. Melmad, L. Laine, and J. M. Henning, Guidelines for the appropriate use of non–steroidal anti–inflammatory drugs, cyclo–oxygenase–2–specific inhibitors and proton pump inhibitors in patients requiring chronic anti–inflammatory therapy, *Ailment Pharmacol. Ther*. **2004**, *19*, 197–208.
[4] S. V. Bhandari, and M. K. Raut, www.pharmainfo.net/exclusive/review/current_advances _in _rheumatoid arthritis_therapy_a _Review.
[5] J. L. Wallance, and A. G. Buret, www.gastro.org/user–asset/documents/08–publications/06–GIHEP_Annual–Review/Articles/Wallace–Buret.pdf.
[6] G. Dannhart, and W. Kiefer, Cyclooxygenase inhibitors – current status and future prospects, *Eur. J. Med. Chem*. **2001**, *36*,109–126.
[7] R. G. Kurumbail, A. M. Stevens, J. K. Gierse, J. J. McDonald, R. A. Stegeman, D. Glide–haus J. M. Miyashiro, T. D. Pening, K. Seibert, P. C. Isakson, and W. C. Stallings, Structural basis for selective inhibition of cyclooxygenase–2 by anti–inflammatory agents, *Nature*. **1996**, *384*, 644.
[8] A. Raz, A. Wyche, N. Siegel, and P. Nedleeman, Regulation of fibroblast Cyclooxygenase synthesis by interleukin–1, *J. Biol. Chem*. **1988**, *263*, 3022–3028.
[9] D. W. Read, W. S. Bradshaw, W. Xie, and D. L. Simmons, In vivo and in vitro expression of a non–mammalian cyclooxygenase–1, *Prostaglandins*. **1996**, *52*, 269.
[10] A. S. Kalguttkar, B. C. Crews, S. W. Rowlinson, C. Garner, K. Seibert, and L. J. Marnett, Aspirin–like Molecules that Covalently Inactivate Cyclooxygenase–2, *Science*.**1998**, *280*, 1268.
[11] N. M. Davies, Toxicity of nonsteroidal anti–inflammatory drugs in the large intestine, *Diseases of colon and rectum*. **1995**, *38*, 1311.
[12] M. D. Murry, and D. C. Brater, Renal Toxicity of the Nonsteroidal Anti–Inflammatory Drugs, *Annu.Rev.Pharm.Toxicol*. **1993**, *33*, 435.
[13] J. H. Botting, Nonsteroidal Antiinflammatory Agents, *Drugs Today* **1999**, 35, 225.
[14] T. D. Penning, J. J. Tally, S. R. Bertenshaw, J. S. Carter, P. W. Collins, S. Doctor, M. J. Graneto, L. F. Lee, J. W. Malecha, J. M. Miyashiro, R. S. Rogers, D. J. Rogier, S. S. Yu, G. D. Anderson, E. G. Burton, J. N. Congburn, S. A. Gregory, C. M. Koboldt, W. E. Perkins, K. Seibert, A. W. Veenhuizen, Y. Y. Zhang, and P. C. Isakson, Synthesis and Biological Evaluation of the 1,5–Diarylpyrazole Class of Cyclooxygenase–2 Inhibitors:# Identification of 4–[5–(4–Methylphenyl)–3–(trifluoromethyl)–1H–pyrazol–1–yl]benzenesulfonamide (SC–58635, Celecoxib), *J. Med. Chem*. **1997**, *40*, 1347.
[15] P. Prasit, Z. Wang, C. Brideau, C. C. Chan, S. Charleson, W. Cromlish, D. Ethier, J. F. Evans, A. W. Ford–Hutchinson, J. Y. Gauthier, R. Gordon, J. Guay, M. Gresser, S. Kargman, B. Kennedy, Y. Leblanc, S. Leger, J. Mancini, G. P. O'Neill, M. Ouellet, M. D. Percival, H. Perrier, D. Riendeau, I. W. Rodger, P. Tagari, M. Therien, P. Vickers, E. Wong, L. J. Xu, R. N. Young, R. Zambani, S. Boyce, N. Rupniak, M. Forest, D. Visco, and D.

Patrick, The discovery of rofecoxib, [MK 966, VIOXX®, 4–(4_–methylsulfonylphenyl)–3– phenyl–2(5*H*)–furanone], an orally active cyclooxygenase–2 inhibitor, *Bioorg*. *Med Chem.Lett*. **1999**, *9*, 1773.

[16] J. J. Talley, D. L. Brown, J. S. Carter, M. J. Graneto, C. M. Koboldt, J. L. Masferrer, W. E. Perkins, R. S. Rogers, A. F. Shaffer, Y. Y. Zhang, B. S. Zweiefel, K. L. Sebert, 4–[5–Methyl–3–phenylisoxazol–4–yl] benzenesulfonamide, Valdecoxib:_A Potent and Selective Inhibitor of COX–2, *J. Med. Chem*. **2000**, *43*, 775.

[17] . J. Talley, S. R. Bertenshaw, D. L. Brown, J. S. Carter, M. J. Graneto, M. S. Kellogg, C. M. Koboldt, J. Yuan, Y. Y. Zhang, and K. Seibert, N–[[(5–Methyl–3–phenylisoxazol–4–yl)–phenyl]sulfonyl]propanamide, Sodium Salt, Parecoxib Sodium: A Potent and Selective Inhibitor of COX–2 for Parenteral Administration, *J. Med. Chem*. **2000**, *43*, 1661.

[18] T. R. Sharpe, S. C. Cherkofsky, W. E. Hewes, D. H. Smith, W. A. Gregory, S. B. Haber, M. R. Leadbetter, and J. G. Whitney, Preparation, antiarthritic and analgesic activity of 4,5–diaryl–2–(substituted thio)–1H–imidazoles and their sulfoxides and sulfones, *J Med. Chem*. **1985**, *28*, 1188–1194.

[19] VLIfeMDS, Molecular Design Suit Version 2.0, V–Life Science TechnologiesPvt.LTD. Pune, Indian, 2004, (www.Vlifesciences.com).

[20] C. Hansch, and A. Leo: In Exploring QSAR, American Chemical Society, Washington, DC, 1995, 19.

[21] S. Ajmani, K. Jadhav, and S. Kulkarni: Three–Dimensional QSAR Using the k–Nearest Neighbor Method and Its Interpretation, *J. Comp*. *Inf. Model*. **2006**, *46*, 24–31.

[22] T. A. Halgren, Merck molecular force field. II. MMFF94 van der Waals and electrostatic parameters for intermolecular interactions, *J. Comp*. *Chem*. **1996**, *17*, 520–552.